π and K fragmentation functions at NNLO

Rabah Abdul Khalek, Valerio Bertone, Alice Khoudli, Emanuele R. Nocera

Fragmentation functions

Fragmentation functions $D_i^h(z) \sim$ probability of finding a given hadron h with momentum fraction z in the products of the fragmentation of a parton i.
They are universal, non perturbatively computable objects (due to encapsulating low-energy behavior of the strong interaction) that appear in the factorization of certain processes.

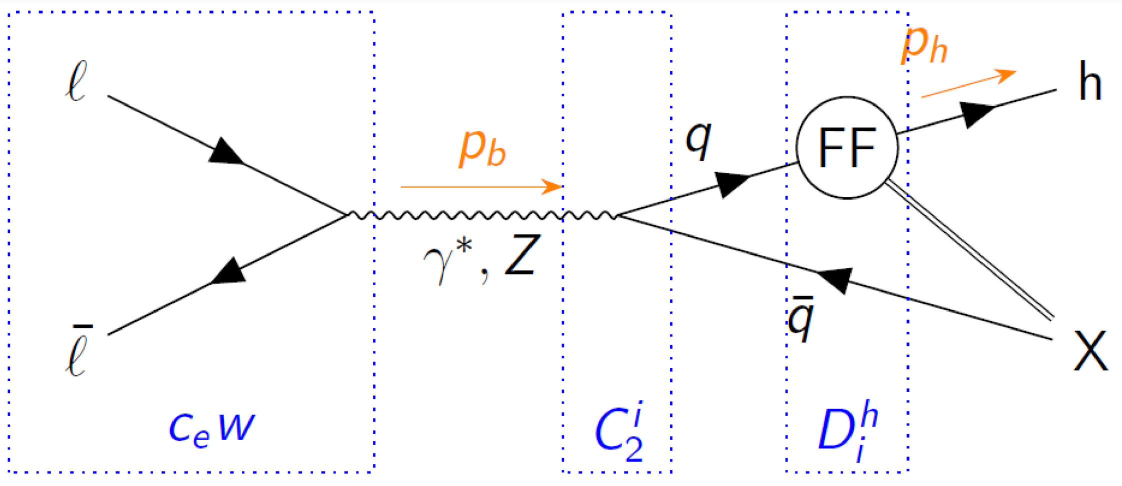

Fig. 1: Single-Inclusive Annihilation

$$Q = p_b^2,\ z = \frac{p_b \cdot p_h}{Q^2}$$

$$\frac{d\sigma_h}{dz}(z,Q) = c_{ew}(Q) \sum_{i=\Sigma,NS,g} C_2^i(z,\alpha_s(Q)) \otimes D_i^h(z,Q)$$

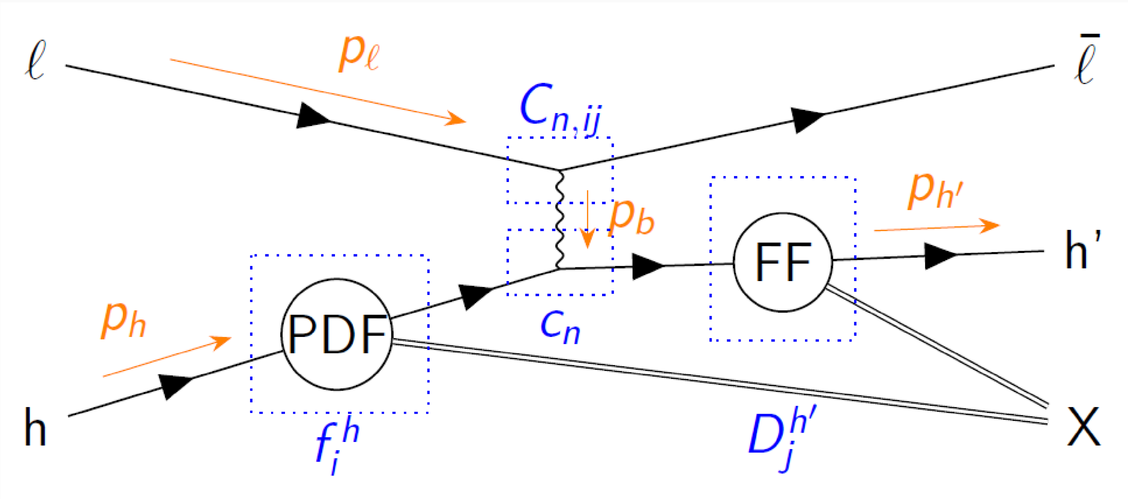

Fig. 2: Semi-Inclusive Deep Inelastic Scattering

$$Q^2 = -p_b^2,\ x = \frac{Q^2}{2 p_h \cdot p_b},\ z = \frac{p_h \cdot p'_h}{p_h \cdot p_b},\ y = \frac{Q^2}{x(p_\ell + p_h)^2}$$

$$\frac{d^3\sigma}{dxdQdz}(z,Q) = \sum_{n=2,L} c_n(Q,y) \sum_{i,j=g,q_f} C_{n,ij}(x,z,Q) \otimes f_i^h(x,Q) \otimes D_j^{h'}(z,Q)$$

DGLAP evolution equations allow us to fit $D_i^h(z,Q)$ at set $Q = \mu_0$

Framework

For each hadron 7 unique flavor combinations of fragmentation functions are fitted, exploiting the charge conjugation and isospin approximate symmetries for sea quarks. They are parametrised using neural networks with a single hidden layer of 20 nodes, a single input node and 7 output nodes. Positivity is imposed by squaring the output, then vanishing at $z = 1$ is imposed by subtraction.
Fitting is performed using Levenberg-Marquardt and the Ceres solver, and cross-validation is used to avoid overfitting.
Experimental uncertainties are propagated using Monte-Carlo sampling.
The APFEL++ evolution code and MontBlanc framework used in this project are publicly available : github.com/vbertone/apfelxx, github.com/MapCollaboration/MontBlanc. The resulting fragmentation function sets are available in MontBlanc and LHAPDF.

Data

SIA data from CERN (ALEPH, DELPHI and OPAL experiments), DESY (TASSO), KEK (BELLE and TOPAZ), and SLAC (BABAR, TPC and SLD).
SIDIS data from COMPASS at CERN and HERMES at DESY.

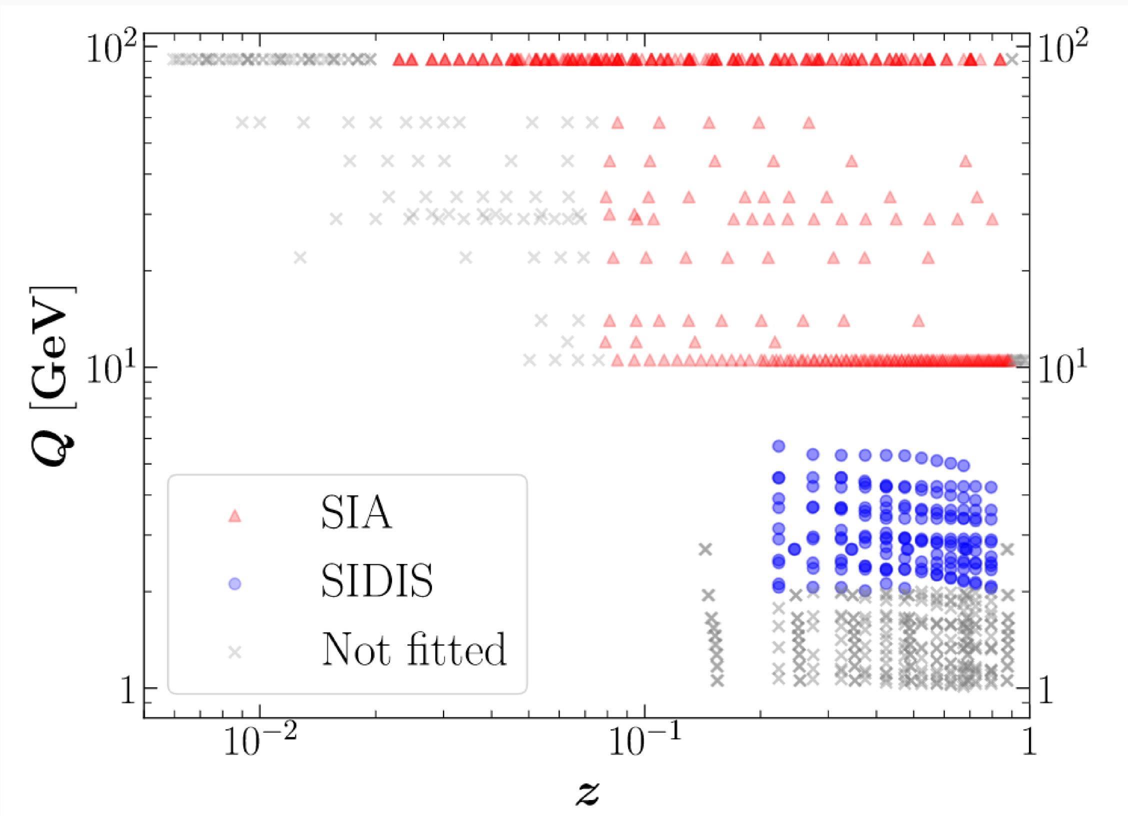

Fig. 3: Kinematic coverage in (z,Q) of included pion data sets. Gray points are excluded by kinematic cuts. Kaon data presents a similar spread, but different kinematic cuts are applied.

From NlO to NNLO

A few months ago M. Abele, D. de Florian, and W. Vogelsang : Approximate NNLO QCD corrections to SIDIS! Our following fits are taking advantage and exploring the impact of those theoretical corrections.

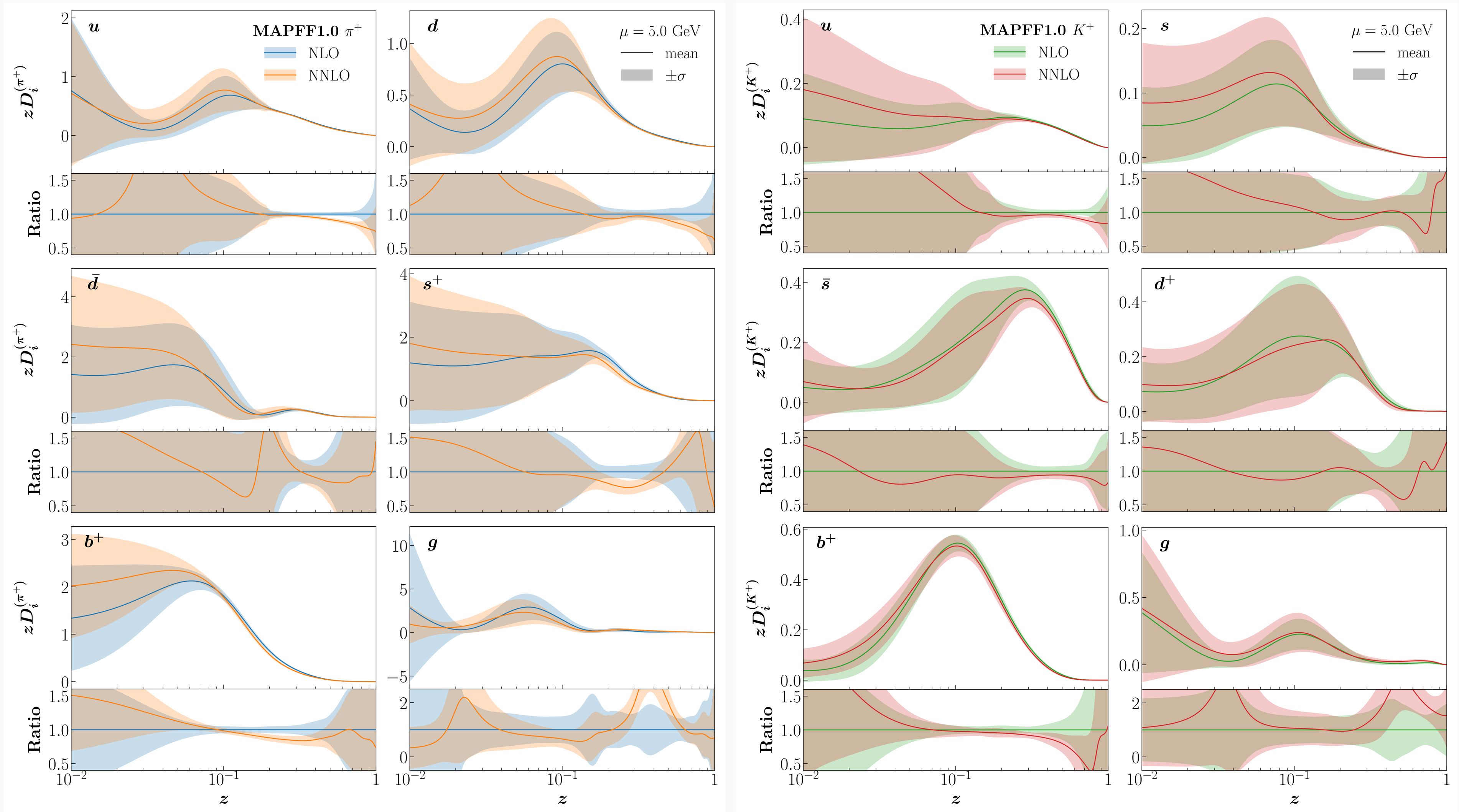

Fig. 4: Left : Comparison of the NLO and NNLO FFs for positively charged pions. We display the $D_u^{\pi+}$, $D_d^{\pi+}$, $D_{\bar{d}}^{\pi+}$, $D_{s+}^{\pi+}$, $D_{b+}^{\pi+}$ and $D_g^{\pi+}$ FFs at $\mu = 5$ GeV. Expectation values and uncertainties correspond to the mean and standard deviation computed over the ensemble of FF replicas. For each FF we plot the absolute distributions in the upper panels and their ratio to the central value of the NLO FFs in the lower ones.
Right : Same for K^+

Experiment	$h=\pi$ N_{dat}	$h=\pi$ χ^2/N_{dat} NLO	$h=\pi$ χ^2/N_{dat} NNLO	$h=K$ N_{dat}	$h=K$ χ^2/N_{dat} NLO	$h=K$ χ^2/N_{dat} NNLO
BELLE $h^\pm$	70	0.14	0.13	70	0.39	0.41
BABAR $h^\pm$	39	0.91	0.76	28	0.36	0.25
TASSO 12 GeV $h^\pm$	4	0.90	0.92	3	0.85	0.87
TASSO 14 GeV $h^\pm$	9	1.33	1.35	9	1.24	1.22
TASSO 22 GeV $h^\pm$	8	1.65	1.81	6	0.89	0.90
TPC $h^\pm$	13	0.23	0.25	13	0.38	0.40
TASSO 30 GeV $h^\pm$	2	0.30	0.34	—	—	—
TASSO 34 GeV $h^\pm$	9	1.08	1.48	5	0.07	0.06
TASSO 44 GeV $h^\pm$	6	1.13	1.37	—	—	—
TOPAZ $h^\pm$	5	0.24	0.37	3	0.10	0.11
ALEPH $h^\pm$	23	1.24	1.46	18	0.49	0.48
DELPHI (inclusive) $h^\pm$	21	1.31	1.25	23	0.97	0.99
DELPHI (uds tagged) $h^\pm$	21	2.68	2.89	23	0.44	0.38
DELPHI (b tagged) $h^\pm$	21	1.58	1.73	23	0.42	0.45
OPAL $h^\pm$	24	1.63	1.79	10	0.39	0.36
SLD (inclusive) $h^\pm$	34	1.05	1.13	35	0.83	0.67
SLD (uds tagged) $h^\pm$	34	1.59	2.16	35	1.37	1.52
SLD (b tagged) $h^\pm$	34	0.55	0.68	35	0.75	0.77
Total SIA	377	1.03	1.15	339	0.58	0.57
HERMES h^- d	2	0.41	0.32	2	0.18	0.13
HERMES h^+ p	2	0.01	0.02	2	0.05	0.04
HERMES h^- d	2	0.17	0.11	2	0.58	0.48
HERMES h^+ p	2	0.35	0.32	2	0.56	0.43
COMPASS h^-	157	0.48	0.55	156	0.74	0.59
COMPASS h^+	157	0.62	0.72	156	0.76	0.67
Total SIDIS	322	0.47	0.52	320	0.64	0.54
Global data set	**699**	**0.68**	**0.76**	**659**	**0.62**	**0.55**

Fig. 5: The number of data points, N_{dat}, and the χ^2 per data point, χ^2/N_{dat}, for each hadronic species and perturbative order considered in the fits of this analysis

Impact of Q_{cut} and correlations of experimental uncertainties

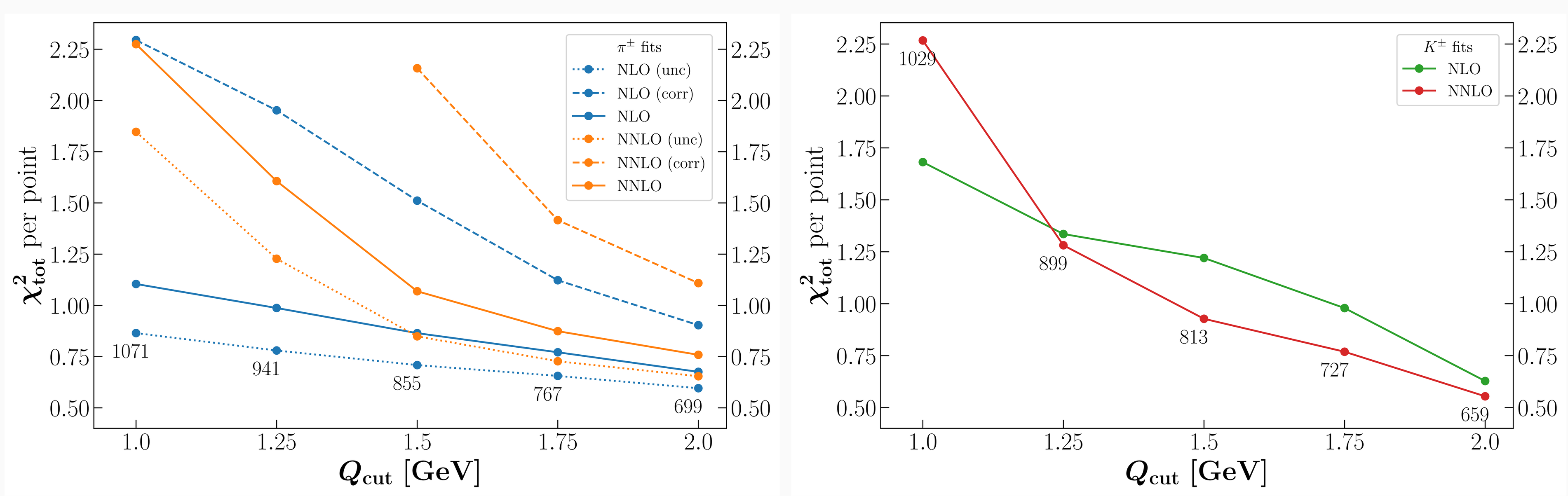

Fig. 6: The value of the total χ^2 per data point as a function of the cut on Q, Q_{cut}, applied to the SIDIS data in the pion (left) and kaon (right) FF fits. For each value of Q_{cut}, the number of data points included in the fits are also displayed. Both NLO and NNLO fits are considered. In the case of the fit of pion FFs, various correlation models for the COMPASS data are taken into account.